**11th International Symposium on Magnetic Bearings**
**August 26-29, Nara, Japan**

# PERFORMANCE IMPROVEMENT OF A SPLIT WINDING BEARINGLESS INDUCTION MACHINE BASED ON A NEURAL NETWORK FLUX OBSERVER

**José Álvaro de Paiva**
Dept. of Inform Technology, Federal Center of Tec. Education of Rio G. do Norte, Natal, R.N, 59015-000, Brazil.
josealvaro@cefetrn.br

**Andrés Ortiz Salazar**
Dept. of Computing Eng. and Automation, Federal University of Rio G do Norte, Natal, R.N, 59072-970, Brazil.
andres@dca.ufrn.br

**André Laurindo Maitelli**
Dept. of Computing Eng. and Automation, Federal University of Rio G do Norte, Natal, R.N, 59072-970, Brazil.
maitelli@dca.ufrn.br

**Richard Magdalena Stephan**
Dept. of Electrical Engineering, Federal University of Rio de Janeiro, Rio de Janeiro, R.J, 21941-972, Brazil
richard@dee.ufrj.br

**ABSTRACT**
This work describes the performance improvement of a 4 poles 1,1 kW split winding bearingless induction machine based on a neural rotor flux observer. The system control executes simultaneously the vector speed control, the radial positioning control and the stator winding current control. The neural flux observer compensates for parameter variations due to temperature changes or due to the rotor magnetic saturation. A program developed in the ANSI C language executes all the system control. The used DSP resources are the Analog/Digital converters, the PWM outputs and the parallel and RS-232 serial interfaces, which are responsible, respectively, for the DSP programming and the data capture through the supervisory system. Comparisons with a fixed parameter observer validate the proposed method.

## 1. INTRODUCTION

In comparison with standard machines, bearingless machines present as advantages: reduction of space and losses, capacity to operate at higher speeds, lower maintenance and application in high vacuum, low temperature and clean atmospheres [1]. Moreover, the split winding bearingless induction machine [2, 3] can be constructed with standard Dahlander motors [4] representing a great cost reduction. The main problem is to guarantee the rotor positioning with an adequate speed control strategy. Under other methods, scheduled adaptive control [5] and linear quadratic regulators [6] have already been tested. In this paper, the premium characteristics of field oriented control, neural networks and DSP numeric processing speed are combined to improve the positioning of a laboratory prototype split winding bearingless induction machine. The machine flux model is revised in chapter 2, the machine structure is presented in chapter 3, the digital system implementation in chapter 4. The laboratory test machine will be described in chapter 5. Finally, experimental results will be presented in chapter 6, followed by the conclusions in chapter 7.

## 2. THE FLUX MODEL

The implemented system is based on the vector control technique that makes the induction machine control similar to the direct-current machine control [7, 8].
The rotor flux referential was chosen to be used in the estimation of the variables related to the rotor. This choice simplifies significantly the digital system implementation. The equations of the rotor flux states are the following:

$$\frac{di_{mR}(t)}{dt} = \frac{i_{sd}(t)}{T_R} - \frac{i_{mR}(t)}{T_R} \tag{1}$$

$$\frac{dr(t)}{dt} = n_p.w_{mec}(t) + \frac{i_{sq}(t)}{T_R i_{mR}(t)} \tag{2}$$

$$m_M(t) = k.i_{mR}(t)i_{sq}(t) \tag{3}$$

$$T_R = \frac{L_R}{R_R} \tag{4}$$

$$k = \frac{2}{3}(1 - s)L_s \quad (5)$$

where:

| | |
|---|---|
| $i_{mR}(t)$ | - Magnetizing current. |
| $i_{Sd}(t)$ | - Field current. |
| $i_{Sq}(t)$ | - Torque current. |
| $\rho(t)$ | - Rotor flux position. |
| $m_M(t)$ | - Electric torque. |
| $n_p$ | - Par poles number. |
| $\omega_{mec}(t)$ | - Rotor mechanical speed. |
| $T_R$ | - Rotor time constant. |
| $R_R$ | - Rotor resistance. |
| $L_R$ | - Rotor inductance. |
| $L_s$. | - Stator inductance. |
| $\sigma$ | - Leakage factor. |

Although simple, this model has nonlinear characteristics and depends directly of the machine parameters. This dependence generates some performance limitations, mainly when these parameters are not well known or change by the influence of external agents as, for example, the temperature or the flux saturation [7,8]. Thus, if some parametric variation occurs, the rotor flux estimation will present an error that can influence the global system performance.
To compensate for the limitations imposed by observers based on models with fixed parameters, this workproposes a flux neural observer composed of two multi layer feedfoward neural networks [9]. These neural networks execute, simultaneously, the rotor flux speed estimation and the magnetization current estimation which defines, respectively, the rotor flux position (after the integration of the flux speed) and the rotor flux magnitude.

## 3. THE SPLIT WINDING BEARINGLESS MACHINE

The winding arrangement of the bearingless induction machine is roughly presented in Figure 1. The currents applied to each winding are given by:

$$i_{A1} = i_A + \Delta i_A \quad (6)$$

$$i_{A2} = i_A - \Delta i_A \quad (7)$$

$$i_{B1} = i_B + \Delta i_B \quad (8)$$

$$i_{B2} = i_B - \Delta i_B \quad (9)$$

$$i_{C1} = i_C + \Delta i_C \quad (10)$$

$$i_{C2} = i_C - \Delta i_C \quad (11)$$

The components $i_A$, $i_B$, $i_C$ give the rotational torque and are established with the field oriented control method. The incremental components $\Delta i_A$, $\Delta i_B$, $\Delta i_C$ are responsible for the positioning and are calculated by two PD controllers and convenient coordinate transformation.

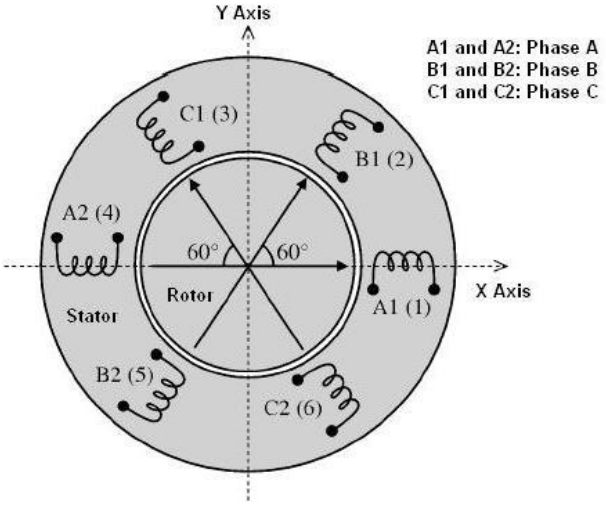


**FIGURE 1:** The basic idea of a split winding bearingless induction machine.

## 4. THE DIGITAL CONTROL SYSTEM IMPLEMENTATION

Figure 2 depicts the block diagram of the complete control system. In this system, the vector speed and radial positioning controllers are guided by the rotor flux observer. The six resultant reference components shown in equations 6-11 are applied to the current controller.
The rotor flux observer, necessary for the field oriented control, is given by two Perceptrons multi layer neural networks (Figure 3).
The networks training was achieved with the off-line back propagation algorithm available at the Matlab Neural Network toolbox. After the training, the neural network weights were normalized for the fix-point operation of the DSP LF2812 [10].
The conventional flux observer was also implemented to provide several comparisons with the neural observer under the same conditions.

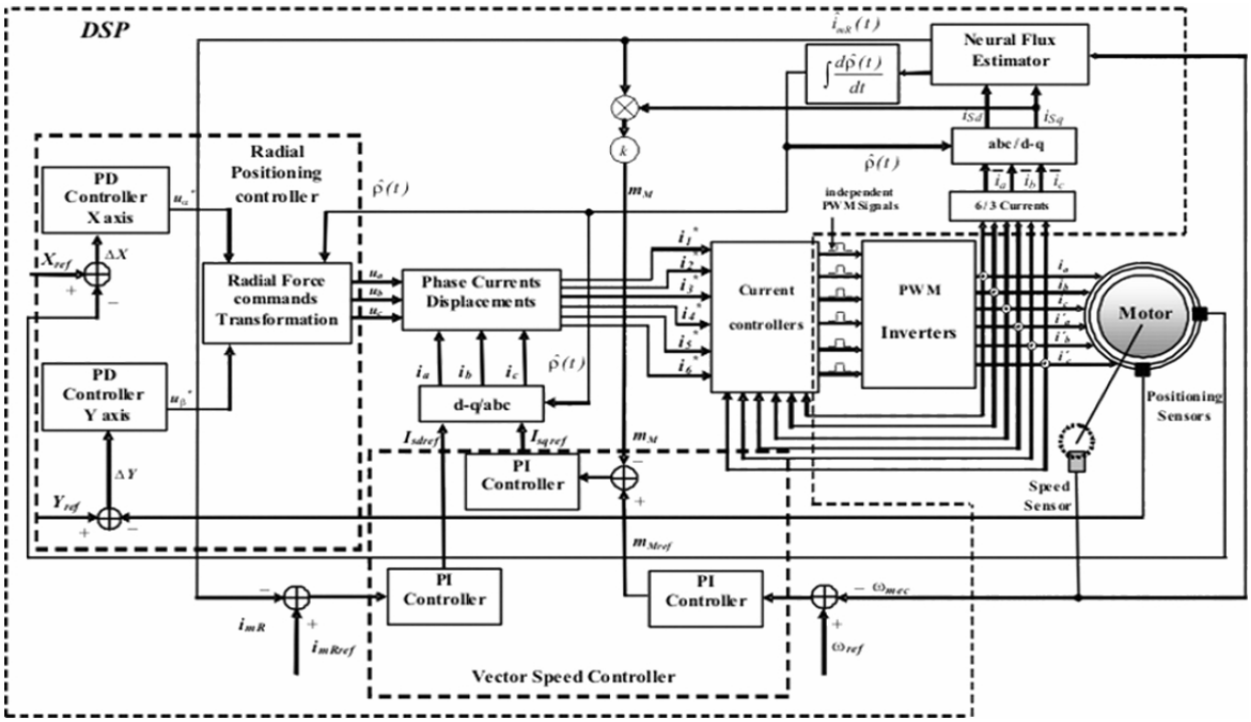


**FIGURE 2:** The complete control system.

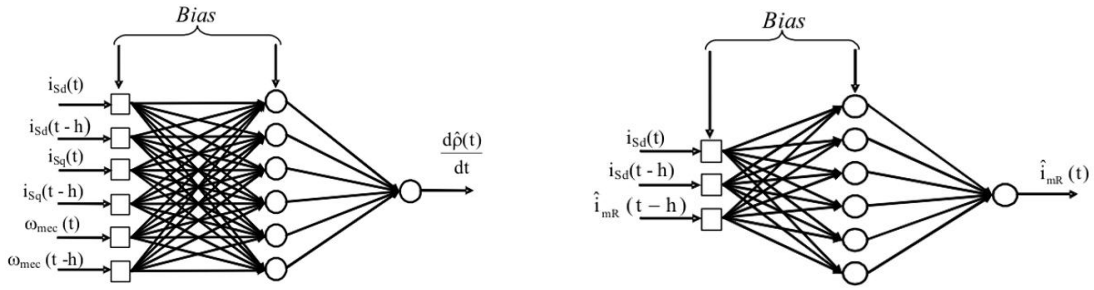


(a) (b)

**FIGURE 3:** Neural networks for the rotor flux velocity (a) and intensity (b) estimation.

## 5. THE LABORATORY PROTOTYPE

Figure 4 shows a picture of the laboratory prototype of 1.1kW.

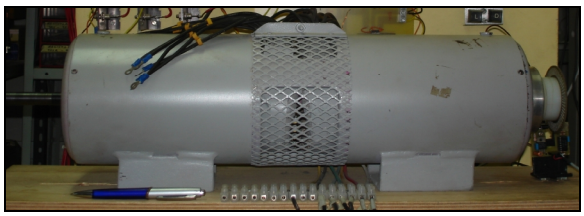

**FIGURE 4:** The laboratory prototype.

The machine parameters were measured in laboratory, and its values are: nominal speed $w_{nom}$ = *1800 rpm*, nominal voltage $V_{nom}$=*220V*, nominal current $I_{nom}$=*1A*, stator resistance $R_S$=*4.5853W*, rotor resistance $R_R$=*32.0894W*, stator and rotor inductance $L_S$=$L_R$=*459.6mH*, magnetizing inductance $L_M$=*278.6mH*, par pole number $n_p$=*2*, inertia moment $J$=*6.06.10*$^{-3}$ *kg.m*$^2$ and leakage factor $s$=*0.1*.

## 6. EXPERIMENTAL RESULTS

The performance of the system described in the previous section was compared with that obtained with

an inverse model flux observer [6] under different test conditions. The tested conditions were the step, the ramp and the disturbance responses.

### 6.1. Step Response

Initially, with the bearingless motor at standstill (x=0.0mm, y=-0.5mm), the speed reference was changed to 1800 rpm. The step response is presented in Figure 5. The positioning obtained with the neural observer improved significantly. The current components $i_{Sd}$ and $i_{Sq}$ also show lower oscillations as can be seen in Figure 6.

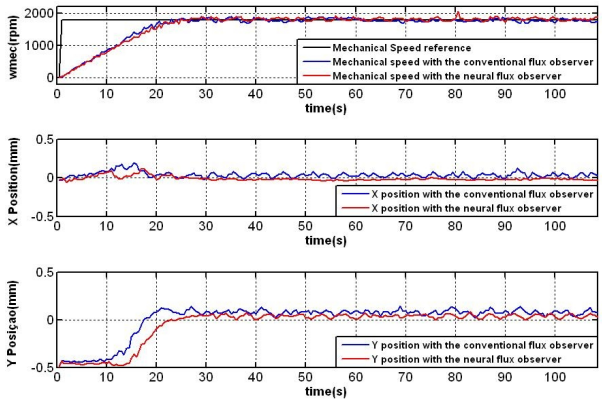


**FIGURE 5:** Step responses of the mechanical speed and X and Y positions.

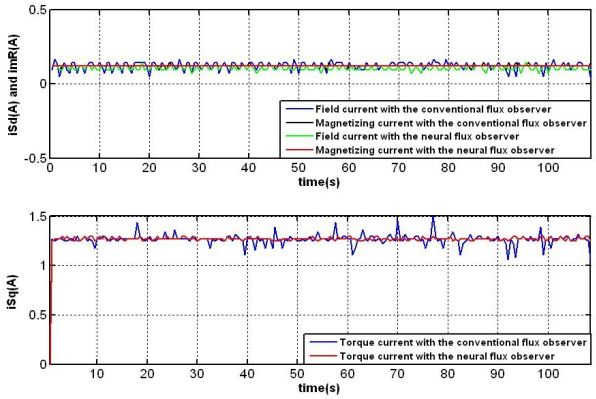


**FIGURE 6:** Field current ($i_{Sd}$), magnetizing current ($i_{mR}$) and torque current ($i_{Sq}$) to the step change.

These current components ($i_{Sd}$ and $i_{Sq}$) are directly responsible for the electric torque generation and one of the main characteristics of this machine type is the strong dependence of the radial positioning in relation to the electric torque, in such a way that, if the electric torque is oscillatory, there will be a significant deterioration of the radial positioning control.

Analyzing the positioning diagram shown in Figure 7, it is possible to confirm that the oscillatory electric torque generated by the control system under the conventional observer orientation results in an oscillatory radial positioning and the X-Y positioning errors in the steady state are larger than the radial positioning errors guided by the neural observer.

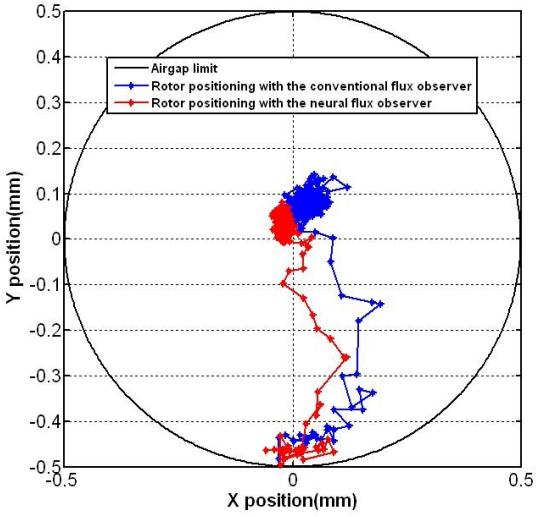


**FIGURE 7:** Radial positioning diagrams with the conventional and neural flux observers to step changes.

### 6.2. Ramp Response

Tests with ramp references were also conducted. Figure 8 shows that the mechanical speed and the X-Y positions of the system operating with the neural observer is faster than the same tests to the system guided by the conventional flux observer errors.

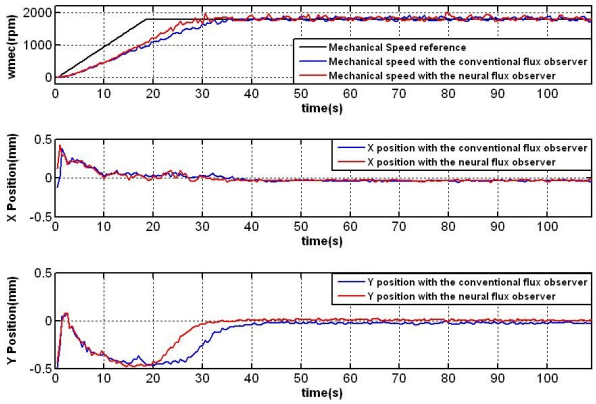


**FIGURE 8:** Ramp responses of the mechanical speed and X and Y positions.

The current components $i_{Sd}$ and $i_{Sq}$ shown in Figure 9 maintain the oscillations presented in the graphs of Figure 6 for the system guided by the conventional observer in relation to the system oriented by the neural observer.

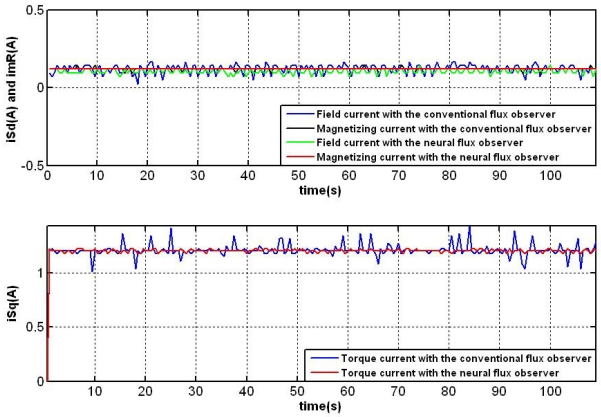


**FIGURE 9:** Field current ($i_{Sd}$), magnetizing current ($i_{mR}$) and torque current ($i_{Sq}$) to the ramp input.

Diagrams shown in Figure 10 confirm the smother behavior and the smaller steady state error of the radial positioning for the system guided by the neural observer.

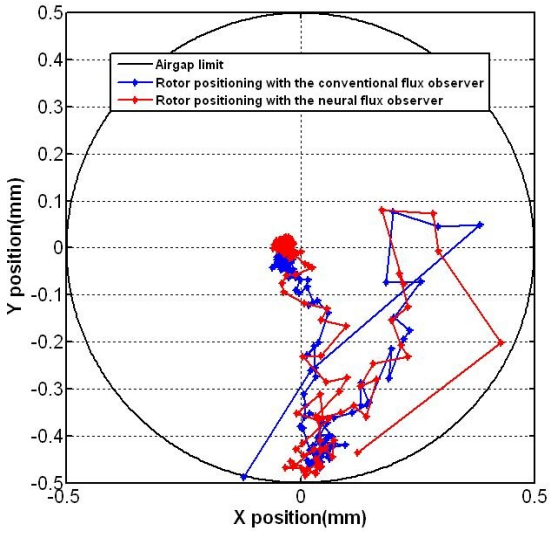


**FIGURE 10:** Radial positioning diagrams with the conventional and neural flux observers to the ramp input.

### 6.3. Disturbance Response

To observe the system behavior under different conditions, tests with slow ramp references and instantaneous load application were accomplished.

The mechanical speed and X-Y position responses presented in Figure 11 show that the applied instantaneous load for the system guided by the neural observer was very close to the load applied during the conventional observer operation.

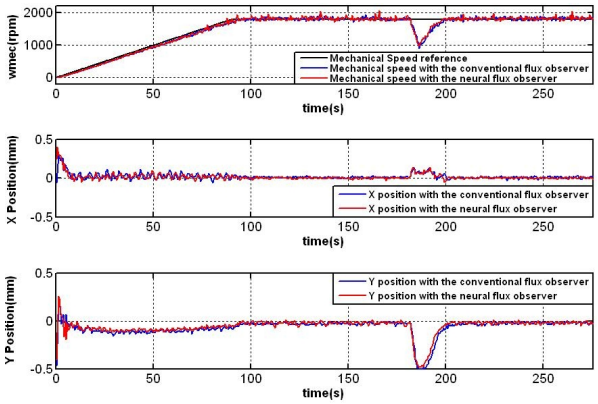


**FIGURE 11:** Ramp responses of the mechanical speed and X and Y positions submitted to an instantaneous load.

The graphs of the mechanical speed $\omega_{mec}$ presented in Figure 11 show that the speed return to the steady state is a little faster when the system is oriented by the neural observer.

For the radial positioning, it is observed that the X and Y responses during the operation of the neural observer follow the references $X_{ref}$ = 0 mm and $Y_{ref}$ = 0 mm with smaller errors than the system operating with the conventional observer to the same load conditions.

The Y responses are the most affected by the load application for both observers operation. However, the return to the steady state for the operation with the neural observer is faster than the response provided by the system guided by the conventional observer.

The currents $i_{Sd}$, $i_{mR}$ and $i_{Sq}$ presented in Figure 12 show a behavior similar to that already seen in the previous tests (Figures 6 and 9), where the conventional observer generated oscillatory responses.

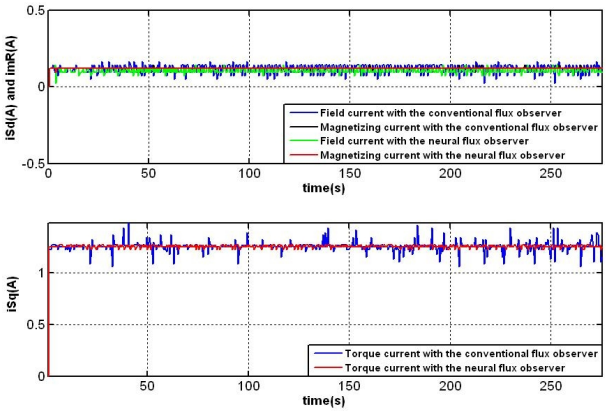


**FIGURE 12:** Field current ($i_{Sd}$), magnetizing current ($i_{mR}$) and torque current ($i_{Sd}$) to the ramp input submitted to an instantaneous load.

In the radial positioning diagrams presented in Figure 13, it is observed that in spite of the deterioration at the X and Y responses due to the instantaneous load application, the rotor axis stays closer to the position references $X_{ref}$ = 0 mm and $Y_{ref}$ = 0 mm when the system is guided by the neural observer.

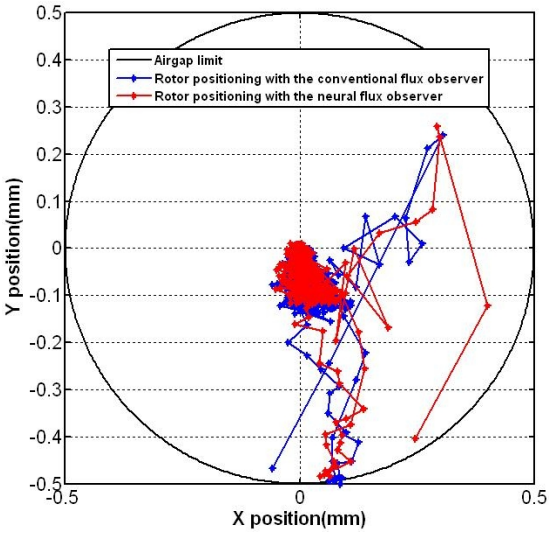


**FIGURE 13:** Radial positioning diagrams with the conventional and neural flux observers to the ramp changes submitted to an instantaneous load.

In agreement with the presented results it was possible to prove that the speed control behavior guided by both observers is very close. However, the neural observer improved significantly the radial positioning control performance.

## 7. CONCLUSION

In the split winding bearingless motor, the rotor positioning and the torque production tasks must be fulfilled with currents flowing trough the same three phase windings. The experimental results of this paper show that a neural network flux observer gives a precise knowledge of the system. Therefore, the positioning can be achieved more easily.

Better results are expected with a motor in the vertical position. In this case, an independent axial bearing will support the rotor weight and the motor winding currents can be left just for the torque production and for small radial positioning efforts.


## ACKNOWLEDGMENT

The authors would to thanks CAPES and CNPq for the financial support.


## REFERENCES


1. Chiba, A., Fukao, T., Ichicawa, O., Oshima, M., Takemoto, M., Dorrel, D. G., "Magnectic Bearings and Bearing Drives", Elsevier, 2005.
2. Salazar, A. O., Dunford, W., Stephan, R. M., Watanabe, E., "A magnetic bearing system using capacitive sensors for position measurement", IEEE Trans. On Magnetics, Vol. 26 Nº 5, pp. 2541-2543, September, 1990.
3. Salazar, A. O., Stephan, R. M., "A bearingless method for induction machine", IEEE Transations On Magnetics**,** Vol. 29, Nº 6, pp. 2965-2967, November, 1993.
4. Chapman, S.J., Electric Machinery Fundamentals, Mc Graw-Hill, New York, 1991.
5. Gomes, R.R., Stephan, R.M., Santisteban, J.A., "Self-Bearing Motor with DSP Based Control System",10th ISMB, Martigny, 21-23 August, 2006.
6. Kauss, W.; Gomes, A.; Stephan, R.M.; David, D. **"**LQR Control of a Bearingless Machine implemented with a DSP**",** 11th ISMB, 2008.
7. Leonhard, W., "30 years space vectors, 20 years field orientation, 10 years digital signal processing with controlled AC drives". EPE-Journal, pp.13, pp. 89, 1991.
8. Leonhard, W., "Control of electrical drives", Springer-Verlag, Third Edition, Berlin Heidelberg New York, Germany, 2001.
9. Lisboa, S. D., Paiva, J. A., Queiroz, F. C. H., Salazar, A. O., Maitelli, A. L., "Neural Flux Estimation Applied to The Vector Speed Control For Induction Machines", 9º Congresso Brasileiro de Eletrônica de Potência", September 30 to October, 04, Blumenau/SC, 2007.
10. Spectrum Digital, "EzDsp LF2812 Technical Reference", DSP development systems, September, 2003.